International Journal of Nanomedicine

Dovepress
open access to scientific and medical research

Open Access Full Text Article

ORIGINAL RESEARCH

One-step mechanochemical preparation and prominent antitumor activity of SN-38 self-micelle solid dispersion

This article was published in the following Dove Medical Press journal:
International Journal of Nanomedicine

Xuanrong Sun
Dabu Zhu
Yue Cai
Guobang Shi
Mengshi Gao
Minzi Zheng

Collaborative Innovation Center of Yangtze River Delta Region Green Pharmaceuticals, Zhejiang University of Technology, Hangzhou 310006, China

Purpose: The purpose of this study was to overcome the clinical defects of 7-ethyl-10-hydroxycamptothecin (SN-38) and explore its characteristics and antitumor effects.

Materials and methods: An amorphous solid dispersion of SN-38 with disodium glycyrrhizin (Na_2GA) was prepared by mechanical ball milling (Na_2GA/SN-38-BM). Moreover, an untreated mixture of Na_2GA and SN-38 (Na_2GA/SN-38-UM), a pure drug SN-38, was prepared for comparison with Na_2GA/SN-38-BM. The samples were characterized by powder X-ray diffraction (PXRD), scanning electron microscopy (SEM), dynamic light scattering, and transmission electron microscopy. Then, further in vitro and in vivo studies were performed including cell uptake, cytotoxicity, antitumor efficacy, tissue distribution, and histopathological evaluation (H&E staining).

Results: SN-38 loaded in Na_2GA was self-formed as nano-micelles in water. The particle size of nano-micelle was 69.41 nm and ζ-potential was −42.01 mV. XRD and SEM analyses showed that the ball milling transformed SN-38 crystals into amorphous form and that solubility increased by 189 times. Compared with SN-38 and Na_2GA/SN-38-UM, Na_2GA/SN-38-BM has a stronger cytotoxicity to tumor cells and exhibited a significant inhibition of tumor growth. Then, pharmacokinetic studies showed that the bioavailability of Na_2GA/SN-38-BM was about four times that of SN-38 suspension.

Conclusion: Na_2GA/SN-38-BM (69 nm, −42 mV) nanoparticles which had excellent pharmacokinetic and distribution properties can dramatically enhance the anticancer efficacy of SN-38 in vitro and in vivo, suggesting a promising formulation for efficient anticancer therapy.

Keywords: SN-38, mechanical ball milling, solid dispersion, antitumor efficacy, pharmacokinetics, tissue distribution, cell-micelle, cytotoxic

Introduction

Irinotecan (CPT-11) and its active metabolite 7-ethyl-10-hydroxyl-camptothecin (SN-38) are both alkaloid-derived topoisomerase I interactive compounds, which exhibit a broad spectrum of antitumor activity.[1,2] CPT-11 can be converted to SN-38 by carboxylesterase-catalyzed hydrolysis that are predominantly present in liver, and SN-38 generated from irinotecan is eventually glycuro-conjugated for metabolic degradation by UGT1A1.[3–5] Owing to its slow hydrolysis rate, irinotecan has an in vitro activity 100- to 1,000-fold lower than SN-38 and also very limited therapeutic efficacy in humans. On the other hand, because of the instability of the active lactone ring, lack of pharmaceutically acceptable excipients, and the extreme insolubility of SN-38,[6–8] its clinical application is markedly restricted.

Several approaches to overcome the problem of SN-38 solubility and bioavailability have been proposed, including incorporation into nanoparticles (NPs),[9,10] liposomes,[11]

Correspondence: Xuanrong Sun
Collaborative Innovation Center of Yangtze River Delta Region Green Pharmaceuticals, Zhejiang University of Technology, No.#18 Chao Wang Road, Hangzhou, China
Tel +86 157 5711 6042
Fax +86 571 8887 1566
Email sunxr@zjut.edu.cn

submit your manuscript | www.dovepress.com
Dovepress
http://dx.doi.org/10.2147/IJN.S193783

polymeric micelles,[12,13] polymer conjugates,[14,15] peptides,[16] carbohydrates,[17] and so on.

In the abovementioned methods, expensive excipients (such as lipids, cholesterol, etc), long time for preparation, complicated process, and various organic solvents (ethanol, dichloromethane, dimethyl sulfoxide, etc) are usually required. Most of these procedures are not environment-friendly and may increase the risk and cost of production. In recent years, mechanochemistry has become an important topic in pharmaceutical research because of its role in green synthesis.[18,19] When solid molecular compounds are subjected to high-energy grinding, their structural and microstructural characteristics as well as their physicochemical stability will vary greatly. The proposed mechanochemical method has significant advantages over traditional "liquid-phase way," and therefore, the bioavailability and solubility will be enhanced and the required dose and side effects will be reduced.

Disodium glycyrrhizinate (Na_2GA) is the salt of glycyrrhizic acid (GA) which can undergo hydrolysis in aqueous solutions and form a free GA. Like GAs, it has anti-inflammatory and anti-cancer properties,[20] and the resulting solution is less viscous and can help improve the solubility and permeability of hydrophobic drugs.[21] Considering the environment-friendly and low-cost mechanochemical techniques and potential dissolution enhancement ability of Na_2GA, an amorphous solid dispersion of SN-38 was prepared by mechanical milling, which was combined with Na_2GA.[22] Moreover, we evaluated the physical characteristics, dissolution law, in vitro and in vivo properties, pharmacokinetics, tissue distribution, and antitumor effects. The main purposes of this study are twofold: 1) to prepare a new dosage form of SN-38 with higher antitumor efficiency by mechanical milling and 2) to study the characterization and behavior of Na_2GA/SN-38-BM in vitro and in vivo.

Materials and methods

Materials

SN-38 was purchased from Shanxi Pioneer Biotech Co. Ltd. (Shanxi, China; purity >99%). Disodium glycyrrhizin (Na_2GA) was purchased from Shanxi Pioneer Biotech Co. Ltd. (Xian, China, purity >98%). Methanol (HPLC grade) was obtained from Tedia Company, Inc (Fairfield, OH, USA). The human lung cancer cell line A549, the human hepatocellular carcinoma cell line $HepG_2$, and the human breast cancer cell line Bcap-37 were purchased from China Center for Type Culture Collection (Wuhan, China).

Male and female Sprague Dawley rats (CD® (SD) IGS) weighing 330–350 g and BALB/c nude mice (6–8 weeks) weighing 18–20 g were obtained from the Shanghai Slac Laboratory Animal Co. Ltd. All the animal experiments in this study were conducted with the approval of the animal experiment center of Zhejiang University of Technology. Animal ethics review number was No. 25/2018. The animal experiments in this study were performed under the guidance of the care and use of laboratory animals in Zhejiang University of Technology (Hangzhou, China) and conformed to the National Institutes of Health Guide for Care and Use of Laboratory Animals (Publication No. 85-23).

Preparation of SN-38 solid dispersion

Roll mill ML007 was used to prepare samples. Briefly, 1 g SN-38 and 100 g Na_2GA were added to 500 mL ball mill pot with three specifications of steel balls (diameter 4, 8, and 12 mm, respectively). The grinding time was 24 hours, and the rotation speed was 20 rpm. Ball milling product was described as Na_2GA/SN-38-BM. Moreover, an untreated mixture of Na_2GA and SN-38 (Na_2GA/SN-38-UM), a pure drug SN-38, was prepared for comparison with Na_2GA/SN-38-BM. Finally, a mixture of SN-38 and GA was prepared by ball milling in the above ratio (GA/SN-38-BM).

Solubility determination

Solubility test was conducted on pure SN-38 and Na_2GA/SN-38-BM. Samples were made into a saturated solution and filtered through a filter paper (0.45 μm). Then, 1 mL filtrate solution was taken out. The filtrate solution was analyzed by an HPLC (Shimadzu LC-20D, Kyoto, Japan) with column Shimadzu ODS-3, 4.6×250 mm at +30°C and ultraviolet-array detector. The eluent was methanol-formate water (80:20, pH 3.0), with flow rate of 1.0 mL/min, and detection wavelength is 380 nm.

Dissolution determination

The dissolution behaviors of SN-38, Na_2GA/SN-38-UM, Na_2GA/SN-38-BM, and GA/SN-38-BM samples were tested in a dissolution tester (RC-6ST; Tianjin, China). The dissolution medium was 900 mL of phosphate buffer (pH 1.2), and the paddle speed was 200 rpm and maintained at 37°C±0.5°C. The doses of four groups were equivalent to 100 mg SN-38. At the set time point, 2 mL of the sample was extracted, and the phosphoric acid medium was added to the container in time. The samples collected in 1 mL vial were treated with methanol and then filtered into liquid phase vials using a syringe with a filter head. Finally, samples were detected using HPLC detector.

Differential scanning calorimetry (DSC)

The prepared samples (3 mg) in hermetically closed aluminum pans using a DSC-250 cell (Thermal Analysis

Co. Ltd., New Castle, DE, USA) were heated from 50°C to the temperature of 30°C higher than melting points at the rate of 10°C/min, and the final temperature was maintained for 10 minutes; rapid temperature drop to 0°C was operated at the rate of −15°C/min. A second heating run was repeated. N_2 was used as protective gas for 50 mL/min. All the data were analyzed using Trios software.

Powder X-ray diffraction (PXRD)

PXRD was performed using Bruker D_2 Phaser diffractometer (Bruker, Germany) by using CuKα radiation to determine SN-38, Na_2GA, Na_2GA/SN-38-BM, and Na_2GA/SN-38-UM. The sampling parameter is the step range 5°–40° at a speed of 2°/min.

Scanning electron microscopy (SEM)

SEM (Nano nova 450, FEI, USA) was used to acquire microphotographs on the surface and cross-section of the samples SN-38, Na_2GA, Na_2GA/SN-38-BM, and Na_2GA/SN-38-UM. Dual adhesive was used to place the four samples onto the metal stubs and then the samples were gold-coated before imaging by electron microscopy.

Particle characterization, zeta potential, and stability

The physicochemical characteristics of the sample that dissolved in water were detected by Zetasizer NanoZS (Malvern Instruments, Malvern, UK). Before being measured, all samples were diluted with physiological saline. The particle size of the nano-micelle, polydispersity index (PDI), and the charge on its surface (ζ-potential) were detected by dynamic light scattering (DLS) and laser Doppler anemometry. The sample was dissolved in PBS. Then the change in particle size and PDI of nano-micelles was detected by DLS for 60 hours.

Determination of the critical micelle concentration (CMC)

Nile red (1 μg) in CH_2Cl_2 (30 μL) was added to a series of vials. After CH_2Cl_2 was evaporated, Na_2GA/SN-38-BM aqueous solutions (3 mL) with various concentrations were added into the vials, stirred for 12 hours. The fluorescence intensity of these solutions was measured by a microplate reader (Flexstation 3; Molecular Devices LLC, Sunnyvale, CA, USA) at the wavelength of 620 nm (excited at 579 nm). The junction of the tangents of the two linear parts of the graph of the fluorescence intensity as a function of Na_2GA/SN-38-BM concentration gave the CMC value.

Transmission electron microscopy (TEM)

Na_2GA/SN-38-BM was configured into 1 mg/mL solution. One drop of solution was dropped on the surface of the copper sheet and the sample was observed by Hitachi H7600 transmission electron microscope (TEM; Hitachi Ltd., Tokyo, Japan).

Multicellular tumor spheroids

Multicellular tumor spheroid models consisting of A549 cancer cell line were prepared by modifying a previously reported protocol.[23] Briefly, 50 μL DMEM containing 1.5% agarose (wt/vol) was plated onto each well of a 96-well microtiter plate under sterile conditions. After the agarose solidifies, the plates were stored at room temperature until use.

The multicellular spheroids of A549 cells were prepared by a hanging drop technique. Generally, cell suspensions were diluted in medium containing 0.24% (w/v) methylcellulose at a density around 10^5 cells per milliliter. Then, 25 μL diluted cells were dropped on the lids of 10 cm cell culture plates. After 24 hours, the spheroids were formed and transferred to agarose-coated 96-well plates with one spheroid in each well. The spheroids were incubated for another 72 hours and obtained multicellular tumor spheroids (400–500 μm in diameter). Subsequently, SN-38, Na_2GA/SN-38-UM, and Na_2GA/SN-38-BM at 10 μg/mL SN-38 concentration were added to the 96-well plate, and the diameter change of each well was determined for a week.

Cellular uptake studies

Fluorescent labeling

Fluorescent labeling dyes, 7 mg curcumin (Frontier Scientific, Inc., Logan, UT, USA), were mixed with 7 mg Na_2GA/SN-38-BM powders and then dissolved in 100 μL tetrahydrofuran completely. About 1 mL distilled water was then added dropwise with continuously stirring for extra 2 hours. Subsequently, 20 kDa MWCO cartridge Spectrum Lab was used for dialysis of the solution. The labeled NPs were stored at −20°C before use.

Na_2GA/SN-38-BM/curcumin localization

Cells were plated on glass bottom dishes (MatTek, Shanghai, China) at a density of 6×10^3 cells per cm^2 and incubated for 24 hours before use. The cells were incubated with 3.5 μg/mL Na_2GA/SN-38-BM/curcumin for 4 hours. Subsequently, after 3× washing with cold PBS, the cells were fixed with 4% formalin for 15 minutes, followed by 1.5 μg/mL DAPI staining at room temperature. The images of cells were acquired

with a Zeiss LSM 510 Meta confocal microscope (confocal laser scanning microscopy [CLSM]; Carl Zeiss Meditech AG, Jena, Germany).

In vitro cytotoxicity studies

The cytotoxicity of SN-38, Na_2GA/SN-38-UM, and Na_2GA/SN-38-BM on human breast cancer cell line Bcap-37, lung cancer cell line A549, and hepatocellular carcinoma cell line $HepG_2$ was determined by MTT cell proliferation assay.[24–26] All the cells were cultivated in the incubator which had a humidified atmosphere containing 5% CO_2 at 37°C. The medium was supplemented with 10% (v/v) FBS and 1% (w/v) penicillin-streptomycin. Bcap-37 cells were cultured in 1,640 medium while A549 and $HepG_2$ cells were cultured in DMEM. In short, ~5,000–10,000 cells per well were evenly plated into 96-well plates and grown overnight.

Meanwhile, the cell-free wells were used as the background, and the wells which implanted cells but with no drug treatment were used as the control group. The media was replaced with different concentrations of SN-38, Na_2GA/SN-38-UM, and Na_2GA/SN-38-BM for 24 hours. Subsequently, 20 μL MTT (5 mg/mL) in PBS was added to each well, and the cells were further incubated at 37°C for 4 hours. Next, the medium containing MTT was removed and 150 μL DMSO was added to each well, and the mixture was shaken at room temperature for 10 minutes to dissolve the formazan crystals produced by living cells. Finally, the optical density of each well was measured at 570 nm using a microplate reader (Flexstation 3; Molecular Devices LLC).

In vivo antitumor efficacy

The antitumor effects of SN-38 suspensions, Na_2GA/SN-38-UM, and Na_2GA/SN-38-BM on Nu/Nu nude mice were further studied. About 0.2 mL of Bcap-37 cells (1×10^6 cells) was injected subcutaneously on mice right flank, and when the tumor volume reached to 50–70 mm^3 (about 7 days after inoculation), they were randomly divided into four groups (n=6/group). Each nude mouse was intragastrically administered with a daily dose of 1 mg/kg equivalent SN-38 concentration, whereas the control group was given a 0.9% saline solution. The width and length of the tumors were measured with a caliper and the mice body weight was weighed every day. Tumor volume was estimated as $[(\text{length})\times(\text{width})^2/2]$.[27] The daily weight of each nude mouse was used as an indicator of systemic toxicity.[28] On the 16th day, the tumors of four groups were dissected, washed with PBS solution, and then weighed. Moreover, tumor paraffin sections of four groups were stained with H&E staining to observe pathological changes.

Pharmacokinetic evaluation

Nine SD rats were randomly divided into three groups including SN-38 suspensions, Na_2GA/SN-38-UM, and Na_2GA/SN-38-BM groups. The dose for each intragastric administration was 1 mg/kg (equivalent to SN-38 concentration). At the set time point, 0.5 mL of blood was taken from the eyelids and placed in the prepared heparinized tube and then centrifuged at 5,000 rpm for 5 minutes. About 100 μL of the upper serum was taken, and 200 μL of methanol and 100 μL of CPT-11 solution (as the internal standard, concentration: 200 ng/mL) were added thereto. The mixture was vortexed for 1 minute, centrifuged at 10,000 rpm for 10 minutes, and then filtered through a syringe with a filter into a liquid vial. Finally, the samples were detected by HPLC.

Tissue biodistribution studies

To investigate the tissue biodistribution of Na_2GA/SN-38-UM, Na_2GA/SN-38-BM, and SN-38 suspensions, three groups of Bcap-37-bearing mice were intragastrically administered with three drugs at dose about 1 mg/kg equivalent to SN-38 before 24 hours. Major organs including heart, kidney, spleen, lung, stomach, liver, and tumors were excised and washed with 0.9% saline before weighed. The organs or tissues were cut into small pieces and homogenized. Tissue homogenate (100 μL) was added with 1 μL of 20% trifluoroacetic acid. SN-38 was extracted with 200 μL ice-cold acetonitrile containing 0.5% acetic acid. The mixture was centrifuged at 12,000 rpm for 10 minutes and 200 μL of the supernatant was transferred to a HPLC sample vial. The drug concentrations in the solutions were determined using HPLC as described above, and the corresponding SN-38 tissue concentrations were calculated accordingly.

Statistical analysis

Data were reported as mean ± SD. Student's *t*-test was used for statistical comparison/analysis. A value of $P<0.05$ was considered statistically significant.

Results and discussion

Solubility and dissolution determination

Through HPLC detection and analysis, the solubility of the pure drug SN-38 was 1.12 μg/mL. Compared with SN-38, the solubility of ball-milling products was increased 189 times. Dissolution profiles of SN-38, Na_2GA/SN-38-UM, Na_2GA/SN-38-BM, and GA/SN-38-BM are shown in Figure 1. Compared with SN-38 and Na_2GA/SN-38-UM, GA/SN-38-BM and Na_2GA/SN-38-BM exhibited better dissolution properties. In PBS solution, GA/SN-38-BM dissolved a little bit faster than Na_2GA/SN-38-BM which had the better solubility. The cumulative amount of SN-38 dissolved after

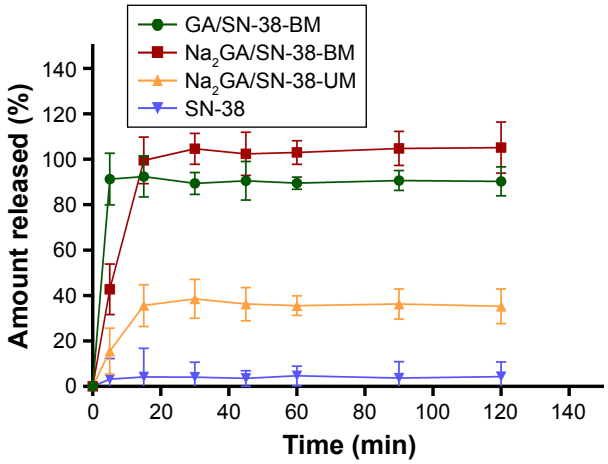

Figure 1 In vitro release profiles of SN-38, Na_2GA/SN-38-UM, Na_2GA/SN-38-BM and GA/SN-38-BM (n=3).
Abbreviations: Na_2GA, disodium glycyrrhizin; Na_2GA/SN-38-UM, untreated mixture of Na_2GA and SN-38; Na_2GA/SN-38-BM, amorphous solid dispersion of SN-38 with Na_2GA)was prepared by mechanical ball milling; SN-38, 7-ethyl-10-hydroxycamptothecin.

5 minutes was 4.2%, 35.6%, 92.5%, and 99.6% for SN-38, Na_2GA/SN-38-UM, GA/SN-38-BM, and Na_2GA/SN-38-BM, respectively. We speculated that the drug was encapsulated in a hydrophilic carrier and formed as the amorphous sample which had better wettability and dispersibility leading to more excellent properties. Na_2GA/SN-38-BM and GA/SN-38-BM form micelles in water, resulting in excellent solubility. While Na_2GA/SN-38-UM was not uniformly dispersed in Na_2GA, therefore only part of SN-38 dissolves rapidly.

Particle size, morphological analysis, and stability

When Na_2GA/SN-38-BM dissolved in water, Na_2GA encapsulated SN-38 to form micelles. The size distribution of the nano-micelles was measured by DLS as shown in Figure 2A. At 25°C, the average particle size has a narrow distribution, which is about 69.41 nm. The PDI value of Na_2GA/SN-38-BM is about 0.255. In addition, the ζ-potential of the particle was −42.01 mV. The CMC was 99.26 μg/mL (Figure 2B). The average particle sizes <200 nm were considered to be at a range suitable to evade filtration in reticuloendothelial system (RES) organs and were more easily absorbed by the tumor.[29] In general, the abovementioned ζ-potential ±30 mV can form a stable dispersion.[30] The negative charge was also proved more easily to evade the RES system's capture so that the tumor tissue can accumulate more drugs. The uniform particle size was further identified by TEM as shown in Figure 2C. The nano-micelles are spherical and have a medium uniform particle size which is consistent with the results measured by DLS. In order to test the stability of the obtained Na_2GA/SN-38-BM NPs, they were suspended in 1× PBS at a concentration of 1 mg/mL, and then the particle size and PDI were monitored by DLS (Figure 2D). The particle size increased from 68 to 81 nm over a span of 60 hours, and the PDI remained relatively the same at 0.26. The change of the particle size indicated that the nano-micelle was relatively stable.

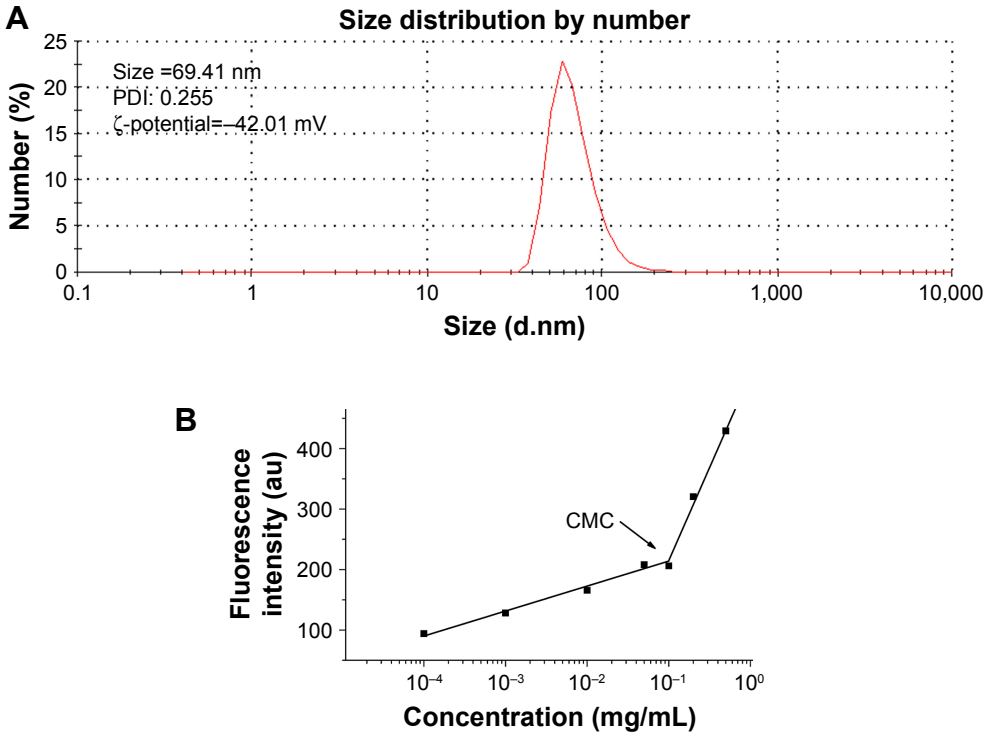

Figure 2 (*Continued*)

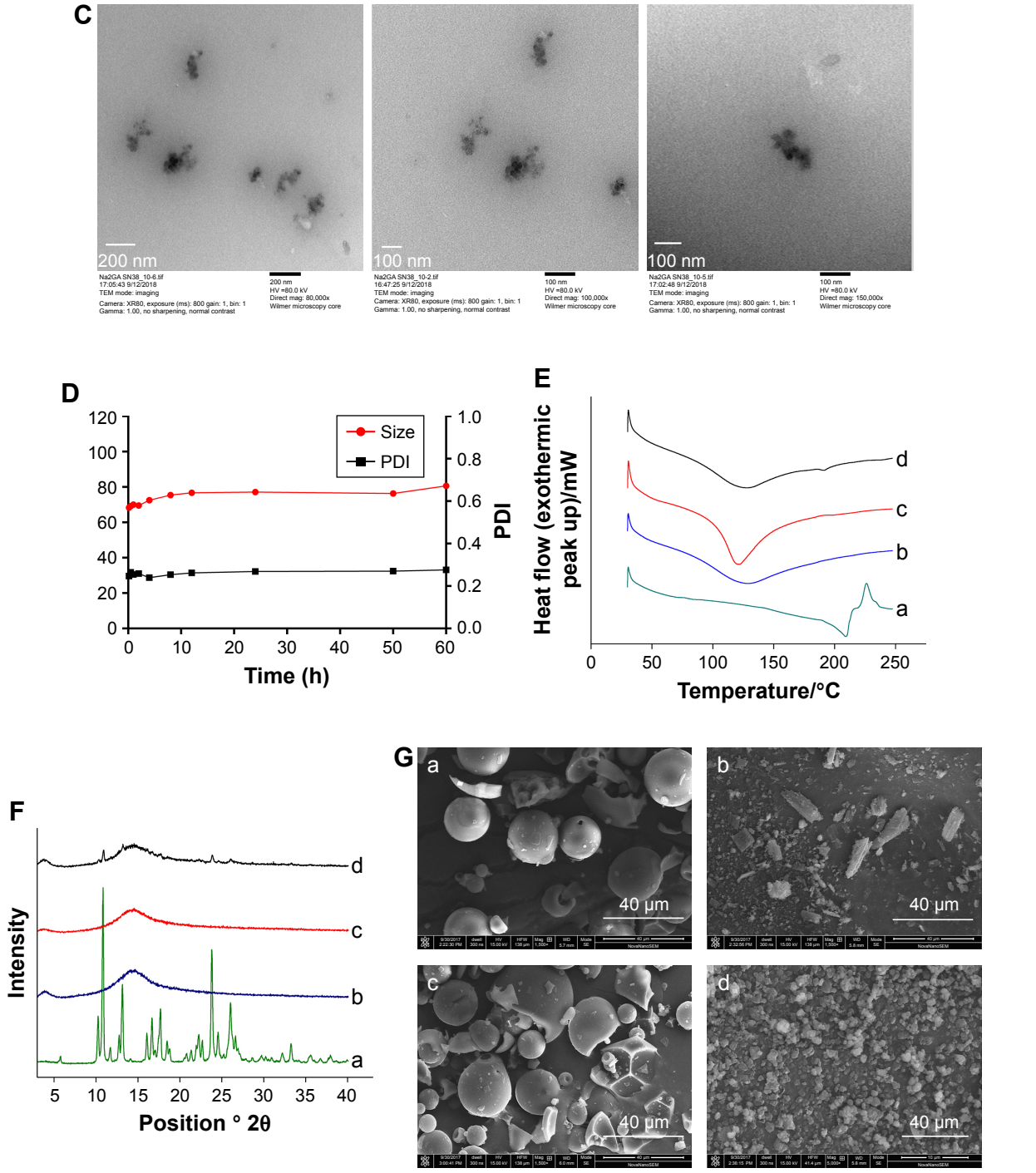

Figure 2 (**A**) Dynamic light scattering size measurement of Na_2GA/SN-38 nanoparticles. (**B**) The CMC value of Na_2GA/SN-38-BM. (**C**) Transmission electron micrograph (TEM) of Na_2GA/SN-38 nanoparticles, the magnification from left to right was 80,000×, 100,000×, 150,000×. (**D**) The stability of Na_2GA/SN-38-BM. (**E**) DSC thermograms of (a) SN-38, (b) Na_2GA, (c) Na_2GA/SN-38-BM, (d) Na_2GA/SN-38-UM. (**F**) X-ray powder diffraction spectra of (a) SN-38, (b) Na_2GA, (c) Na_2GA/SN-38-BM, (d) Na_2GA/SN-38-UM. (**G**) The electron micrographs of (a) Na_2GA, (b) SN-38, (c) Na_2GA/SN-38-UM, (d) Na_2GA/SN-38-BM.
Abbreviations: CMC, critical micelle concentration; PDI, polydispersity index.

Crystalline state analysis

The DSC thermograms of Na_2GA, SN-38, Na_2GA/SN-38-UM, and Na_2GA/SN-38-BM are shown in Figure 2E. The DSC curves of SN-38 exhibited endothermic peaks around 215°C and a characteristic peak was at 200°C–250°C. There was also a characteristic peak observed in Na_2GA/SN-38-UM, but the peak intensity of Na_2GA/SN-38-BM disappeared. It was speculated that SN-38 had been transformed into an amorphous state during the mechanical grinding process, and therefore, SN-38 had been uniformly distributed in Na_2GA.

The PXRD thermograms of Na_2GA, SN-38, Na_2GA/SN-38-UM, and Na_2GA/SN-38-BM are shown in Figure 2F.

The characteristic peak 2θ values of SN-38 were detected to be 10.40, 10.96, 13.24, 17.75, 23.90, and 26.10, indicating that it was a crystal. In the Na_2GA/SN-38-UM diffraction spectrum of the physical mixture, the characteristic crystallization peak of SN-38 was significantly decreased, and no characteristic peaks were found in the Na_2GA/SN-38-BM after grinding for 24 hours. From the diffraction pattern of Na_2GA/SN-38-BM and the DSC thermograms, we can further identify that SN-38 was dispersed in Na_2GA to form an amorphous sample by physical ball milling.

Electron micrographs of SN-38, Na_2GA, Na_2GA/SN-38-UM, and Na_2GA/SN-38-BM are shown in Figure 2G. It could be visually seen that SN-38 was elongated and the Na_2GA was in a spherical state. However, after 24 hours of mechanochemical milling, the intact morphology of the SN-38 and Na_2GA particles was destroyed, forming fine and irregularly shaped particles. Grinding made the particles more uniform, which increased the surface area of the particles, thereby increasing the rate of dissolution.

In vitro cellular studies and cytotoxicity

The colocalization and internalization by A549 cells of Na_2GA/SN-38-BM/curcumin was confirmed by CLSM. As shown in Figure 3A, the fluorescence from Na_2GA/SN-38/curcumin (green) was observed in the cytoplasm after 4 hours of incubation at 37°C, indicating that Na_2GA/SN-38/curcumin was quickly taken up by A549 cells and located in cytoplasm of the tumor cells.

The cytotoxicity of SN-38 suspensions, Na_2GA/SN-38-UM, and Na_2GA/SN-38-BM was evaluated in cancerous A549, Bcap-37, and $HepG_2$ cell lines by MTT assay. As shown in Figure 3B, compared with SN-38 suspensions, Na_2GA/SN-38-UM and Na_2GA/SN-38-BM have the significant inhibition ability in all three cancer cell lines. The half maximal inhibitory concentrations (IC50) of Na_2GA/SN-38-BM and Na_2GA/SN-38-UM were 1.25 and 4.71 μg/mL on Bcap-37 cells, 1.30 and 1.77 μg/mL on A549 cells, and 1.62 and 2.18 μg/mL on $HepG_2$ cells, respectively. Compared with SN-38 suspension, the comparison was statistically significant ($P<0.05$). Furthermore, Na_2GA/SN-38-BM and Na_2GA/SN-38-UM were two or three times stronger than SN-38 suspension ($P<0.05$). Therefore, Na_2GA/SN-38-BM enhanced the cytotoxic ability of SN-38. In addition, all obtained cytotoxic action of Na_2GA/SN-38-BM was due to the SN-38 effect. As shown in Table 1, the survival rate of all three cell lines was above 90%, which confirmed that Na_2GA itself possessed no cytotoxicity in all tested cell lines in the concentration range of 50–200 μg/mL.

There are some possible explanations for these results. First, the lactone ring of SN-38 is prone to hydrolysis at pH 7.4,[31] and the stability of the lactone ring in Na_2GA/SN-38-BM NPs might be enhanced significantly compared to the solution.[26,32] Second, SN-38 is a P-gp substrate.[33] Part of SN-38 molecules in tumor cells will be effluxed outside cells by P-gp transporters, while Na_2GA/SN-38-BM NPs is not affected by P-gp transporters due to its pinocytosis pathway to enter the cells.[34] Finally, mechanical ball milling and Na2GA significantly increase the solubility of the drug. Excess Na2GA/SN-38-BM and pure drug SN-38 dissolved the same dose of water, and Na2GA/SN-38-BM gave a modified concentration of SN-38. All these reasons might explain the enhancement of cytotoxicity of Na_2GA/SN-38-BM NPs.

Further multicellular tumor spheroids were used to investigate NP cytotoxicity in 3D models. As shown in Figure 3C, apart from untreated group, SN-38 suspensions and Na_2GA/SN-38-BM treatment groups both decreased the spheroid diameter, and there was a similar downward trend. The relative diameter of SN-38 group dropped to about 25%, and the Na_2GA/SN-38-BM group dropped to about 46% (Figure 3D). It maybe is due to their cytotoxic effects on A549 cells. Moreover, compared with SN-38 group, a large number of dead cells were seen in the MCTSs of Na_2GA/SN-38-BM groups.

In vivo antitumor efficacy

Next, we investigated the antitumor effects of SN-38 suspensions, Na_2GA/SN-38-UM, and Na_2GA/SN-38-BM on nude mice bearing Bcap-37 tumors. Each nude mouse was intragastrically administered with a daily dose of about 1 mg/kg equivalent to SN-38, and the control group was given a 0.9% saline solution. Animal body weight and tumor size were monitored every day. As shown in Figure 4A and C, compared with the control group, Na_2GA/SN-38-BM showed better tumor inhibition ability throughout the treatment, nearly 53.70% tumor inhibitory rate. Meanwhile, Na_2GA/SN-38-UM and SN-38 suspensions showed no significant differences compared with the control group ($P<0.001$ for Na_2GA/SN-38-BM).

The potential systemic toxicities of different SN-38 formulations to nude mice were assessed based on changes in body weight (Figure 4B). Two days after the start of intragastric administration, mild diarrhea occurred in the nude mice treated with the SN-38 suspensions. Compared with the control group, the treatment group had mild weight loss (<10%) during intragastric administration and recovered after ~5 days. The mice treated with Na_2GA/SN-38-UM exhibited slightly more body weight loss after 15 days (about 1 g). Meanwhile, the mice in the Na_2GA/SN-38-BM treatment groups did not lose weight, but increased slightly. This result indicates that the severe side effects caused by the formulation can be negligible at the test dose.

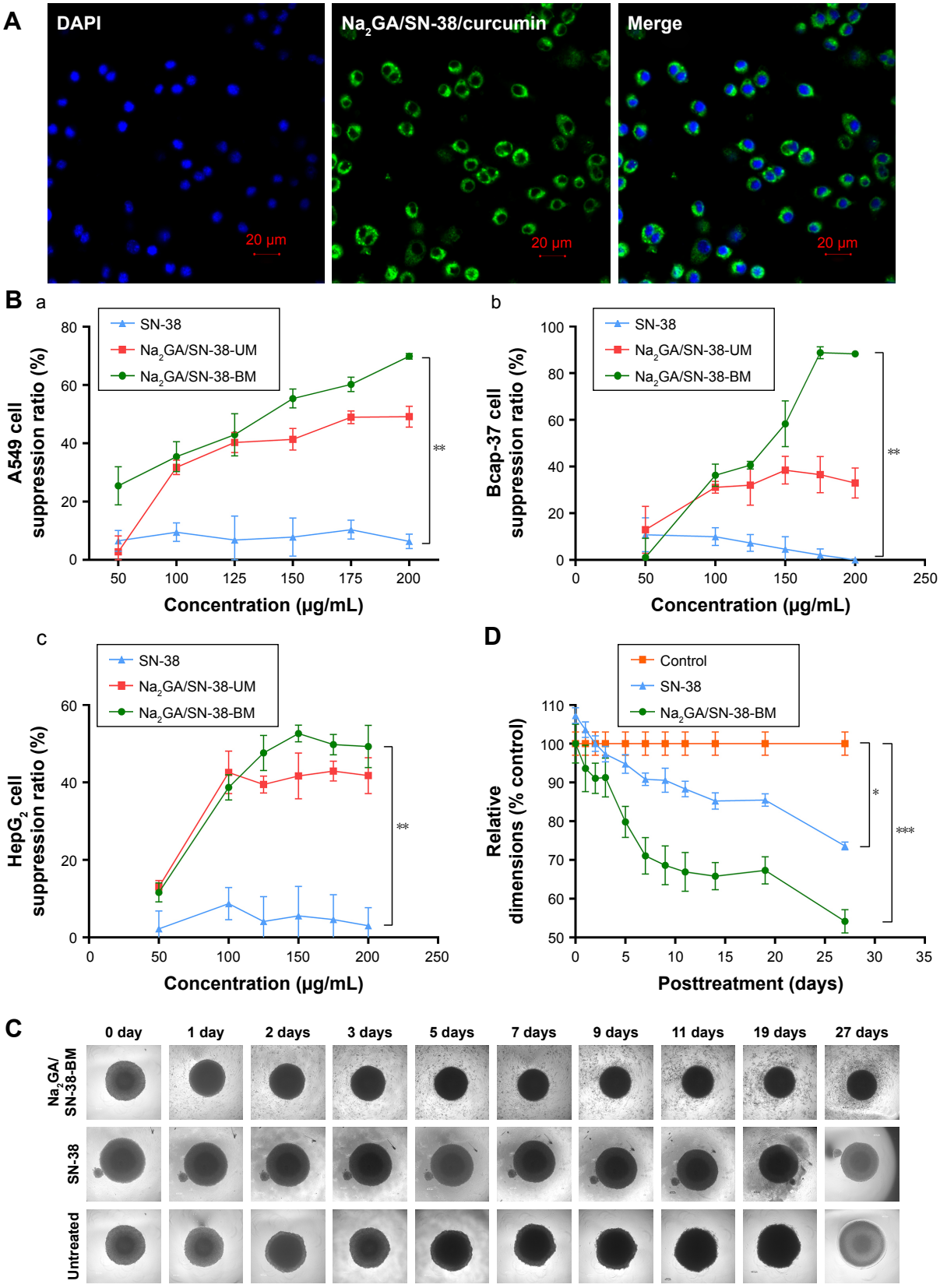

Figure 3 (**A**) Cell uptake of Na_2GA/SN-38-BM/Curcumin. Nucleus was stained with DAPI. Images were taken from the DAPI channel (blue), Na_2GA/SN-38-BM/Curcumin channel (green), and the overlapped image. (**B**) In vitro cytotoxicity of SN-38, Na_2GA/SN-38-UM and Na_2GA/SN-38-BM. (a) suppression ratio on A549 cells, (b) suppression ratio on Bcap-37 cells, (c) suppression ratio on HepG2 cells (n=3). (**C**) Image-based quantification of the relative average diameter of untreated and treated cells spheroids, The image of multicellular tumor spheroids. (**D**) Data represent the average of n≥20 cell spheroid (±SEM). *P<0.05, **P<0.01, and ***P<0.001, compared with untreated group.
Abbreviations: Na_2GA, disodium glycyrrhizin; Na_2GA/SN-38-UM, untreated mixture of Na_2GA and SN-38; Na_2GA/SN-38-BM, amorphous solid dispersion of SN-38 with Na_2GA) was prepared by mechanical ball milling; SN-38, 7-ethyl- 10-hydroxycamptothecin.

Table 1 Cytotoxicity of Na_2GA in A549, Bcap-37, and $HepG_2$ cell lines

Concentration of Na_2GA, μg/mL	Viability, %		
	A549	Bcap-37	$HepG_2$
50	95.1±2.13	96.4±2.07	91.3±2.18
100	93.4±2.17	96.9±2.75	93.0±1.43
125	95.1±3.54	95.5±1.73	94.8±2.55
150	94.3±1.27	93.7±2.99	93.3±2.60
175	95.0±4.27	93.1±1.97	94.1±1.10
200	98.4±2.91	96.1±1.41	95.2±3.21

Note: Values are presented as mean viability ± SEM.
Abbreviations: A549, human lung cancer cell line; Bcap-37, human breast cancer cell line; $HepG_2$, human hepatocellular carcinoma cell line; Na_2GA, disodium glycyrrhizin; SEM, standard error of the mean.

On the 16th day, the tumors of the four groups of nude mice were dissected and washed with 0.9% saline and then weighed to calculate the tumor inhibition rate (IR) (Figure 4C). The average tumor weight of the group administered with saline, SN-38 suspensions, Na_2GA/SN-38-UM, or Na_2GA/SN-38-BM was 0.54, 0.52, 0.38, or 0.25 g, respectively. The IR of SN-38 suspensions, Na_2GA/SN-38-UM, or Na_2GA/SN-38-BM groups was 3.70%, 29.63%, or 53.70%, respectively, relative to the control group.

The tumor tissue sections were subjected to H&E staining, and the pharmacological and toxicological effects of the three groups on the tumor cells were observed. From Figure 4D, we could find that the cells of control group were dense and had abundant vascular tissue. However, different degrees of apoptosis were seen in tumors treated with SN-38 suspension, Na_2GA/SN-38-UM, and Na_2GA/SN-38-BM. Especially in the Na_2GA/SN-38-BM group, a large amount of excessive vacuolization was observed in the tissue sections. This indicated that Na_2GA/SN-38-BM was the most cytotoxic. The result was consistent with the above tumor inhibition data. In summary, the antitumor effect of Na_2GA/SN-38-BM is the most prominent of the three formulations.

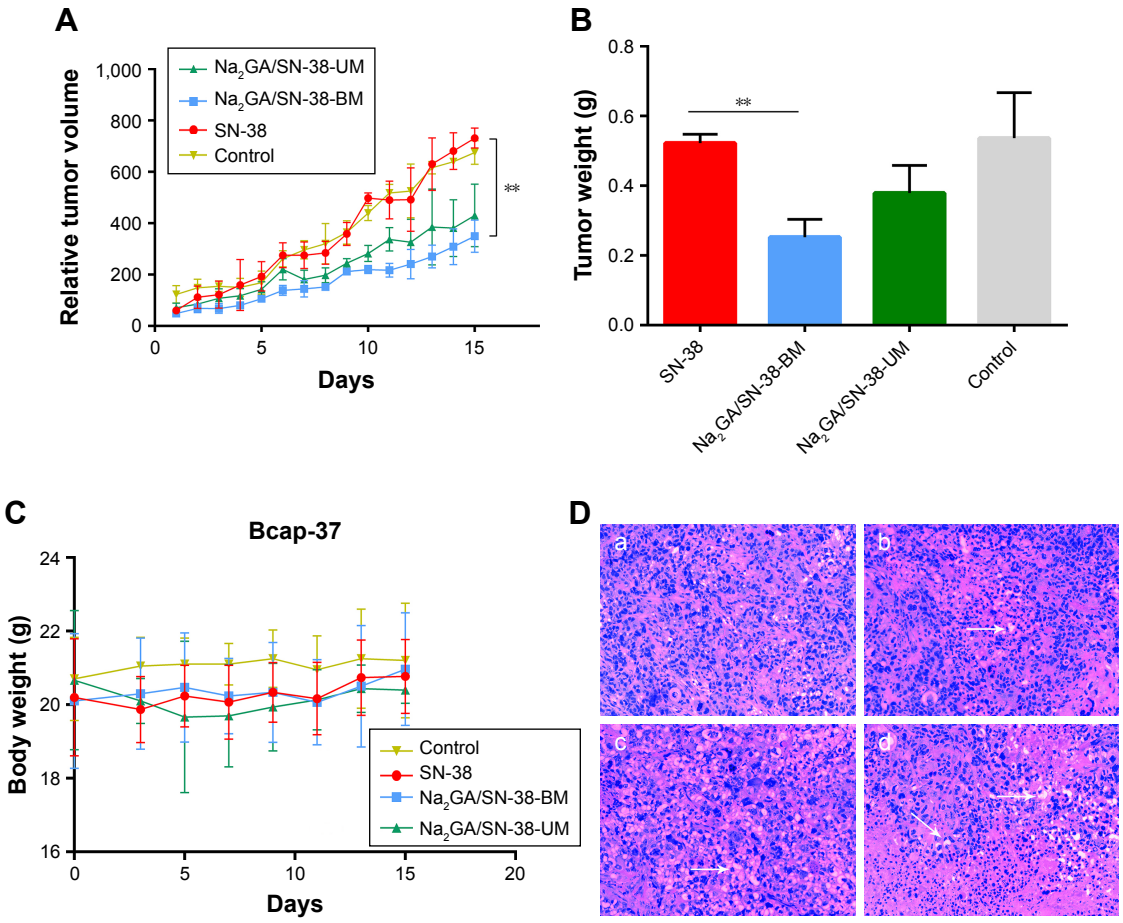

Figure 4 In vivo antitumor effect tested in Bcap-37-bearing mice (n=6). SN-38 suspensions, Na_2GA/SN-38-UM and Na_2GA/SN-38-BM were intragastric administration to mice at the dose of 100 mg/kg, and 0.9% saline was used as control. (**A**) The profile change of tumor volume. $^{**}P<0.01$, Na_2GA/SN-38-BM group compared with SN-38 group. (**B**) The body weight curve of mice. $^{**}P<0.01$, Na_2GA/SN-38-BM group compared with SN-38 group. (**C**) Mean weight of tumors in each group upon animal termination. (**D**) H&E staining of tumor tissue sections. Tumor paraffin sections dyed with H&E reagent were well prepared for observation of the pathological change separately under the microscope (×200). The mice were administered (a) 0.9% saline, (b) SN-38 suspensions, (c) Na_2GA/SN-38-UM, and (d) Na2GA/SN-38-BM.
Abbreviations: Na_2GA, disodium glycyrrhizin; Na_2GA/SN-38-UM, untreated mixture of Na_2GA and SN-38; Na_2GA/SN-38-BM, amorphous solid dispersion of SN-38 with Na_2GA) was prepared by mechanical ball milling; SN-38, 7-ethyl- 10-hydroxycamptothecin.

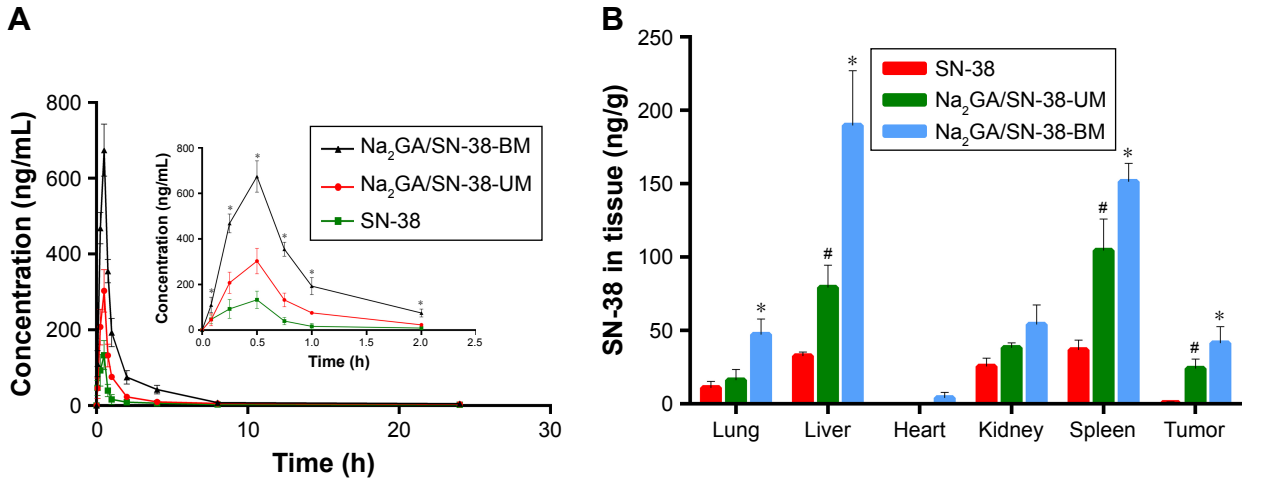

Figure 5 (**A**) Concentration of SN-38 in rat plasma after intragastric administration of SN-38 suspensions, Na_2GA/SN-38-UM and Na_2GA/SN-38-BM to rats at the dose of 1 mg/kg (n=3), *P<0.05, statistical signifcance compared to SN-38 suspensions. (**B**) Biodistribution of SN-38 in Bcap-37-bearing mice after 24 h treatment with SN-38, Na2GA/SN-38-UM and Na_2GA/SN-38-BM (n=3). *P<0.05, Na_2GA/SN-38-BM vs SN-38, #P<0.05, Na_2GA/SN-38-UM vs SN-38.
Abbreviations: Na_2GA, disodium glycyrrhizin; Na_2GA/SN-38-UM, untreated mixture of Na_2GA and SN-38; Na_2GA/SN-38-BM, amorphous solid dispersion of SN-38 with Na_2GA) was prepared by mechanical ball milling; SN-38, 7-ethyl- 10-hydroxycamptothecin.

Pharmacokinetics study

The SN-38 blood concentration–time curves are depicted as Figure 5A. It could be clearly seen from the figure that Na_2GA/SN-38-BM had the better bioavailability compared with Na_2GA/SN-38-UM and SN-38. After intragastric administration, SN-38 distributed rapidly into the whole body and reached the highest blood concentration at 0.5 hour, after that SN-38 distributed to the whole body and cleared slowly and finally expelled from the body at about 2 hours. As shown in Table 2, the bioavailability of the SD rats treated with SN-38 suspensions, Na_2GA/SN-38-UM, and Na_2GA/SN-38-BM were 212, 351, and 818 μg/L*h, respectively. Compared with the SN-38 suspension, the area under the curve of Na_2GA/SN-38-BM increased about four times larger, and the maximum blood concentration increased about five times higher.

There were several reasons that could explain the increase in bioavailability of Na_2GA/SN-38-BM. First, it is well known that the bioavailability of the solution was the best, followed by suspension, and powder was worst.[35] In water, Na_2GA/SN-38-BM formed a homogeneous solution by forming nano-micelles. Some of SN-38 and Na_2GA/SN-38-UM samples could not dissolve completely. So the bioavailability was worse than Na_2GA/SN-38-BM. Second, the crystalline vs amorphous properties (SN-38 and Na_2GA/SN-38-BM) might also play a role. The drug encapsulated in a hydrophilic carrier formed as the amorphous sample which had better wettability and dispersibility, and thus had more excellent pharmacokinetics properties. Third, it was reported that GA increases drug permeability not only due to increased solubility but also due to increased drug permeability through cell membranes.[20,36] Na_2GA has similar properties to GA and can penetrate more into the cells than SN-38 suspension, therefore leading to a better bioavailability.

SN-38 biodistribution in tumor-bearing mice

The concentration of SN-38 in tumors and major organs of the heart, liver, spleen, lungs, and kidneys were studied after three groups of different formulations administered intragastrically at a dose of about 1 mg/kg equivalent to

Table 2 Pharmacokinetic parameters after intragastric administration of SN-38 suspensions, Na_2GA/SN-38-UM, and Na_2GA/SN-38-BM at a dose of 100 mg/kg in Sprague Dawley rats (n=3)

Parameters	SN-38 solution	Na_2GA/SN-38-UM	Na_2GA/SN-38-BM
C_{max} (μg/L)	133.30	303.03	674.20*
T_{max} (h)	0.5	0.5	0.5
$T_{1/2}$ (h)	2.08	2.87	2.96
$AUC_{0\to t}$ (μg/L*h)	151.56	338.84	818.05**
$AUC_{0\to\infty}$ (μg/L*h)	212.47	350.62	818.09*

Note: *P<0.05 and **P<0.01, statistical significance compared to SN-38 suspensions.
Abbreviations: AUC, area under the plasma concentration–time curve; C_{max}, peak plasma concentration; Na_2GA; disodium glycyrrhizin; Na_2GA/SN-38-UM, untreated mixture of Na_2GA and SN-38; Na_2GA/SN-38-BM, amorphous solid dispersion of SN-38 with Na_2GA prepared by mechanical ball milling; SN-38, 7-ethyl-10-hydroxycamptothecin; T_{max}, time to reach peak concentration.

SN-38. As shown in Figure 5B, SN-38 in the formulation of Na_2GA/SN-38-BM can be detected in the abovementioned organ tissues after 24 hours. The amount of SN-38 in the tumors administered with SN-38 suspensions was almost undetectable, and the drug accumulated in the tumors treated with Na_2GA/SN-38-UM and Na_2GA/SN-38-BM was 32- and 56-fold higher than that treated with SN-38 suspensions, respectively. The amount of SN-38 accumulated in liver and spleen of the mice treated with Na_2GA/SN-38-UM and Na_2GA/SN-38-BM was remarkably higher than that treated with SN-38 suspensions. In addition, the average particle sizes of <200 nm were considered to be at a range suitable to evade filtration in RES organs. The nano-micelles size of Na_2GA/SN-38-BM formed in water was about 69 nm, which can prolong the residence time in the blood. Na_2GA/SN-38-UM could also form part of nano-micelles. Therefore, the formulations of Na_2GA/SN-38-UM and Na_2GA/SN-38-BM have better tumor inhibition than SN-38 suspensions.

Conclusion

In this study, Na_2GA/SN-38-BM was successfully developed by mechanical ball milling and overcame the clinical defects of SN-38. Crystalline state analysis showed that SN-38 was uniformly dispersed in the hydrophilic carrier and became amorphous in physical ball milling. Compared with conventional physical mixture, the dissolution of SN-38 was increased markedly after grinding. SN-38-loaded nano-micelles were self-formed by Na_2GA when Na_2GA/SN-38-BM dissolved in water. Compared with SN-38 and Na_2GA/SN-38-UM, Na_2GA/SN-38-BM showed good properties in vitro and in vivo, significantly improving the antitumor effect of SN-38. In Bcap-37 tumor-bearing mice, the antitumor effect of Na_2GA/SN-38-BM was better than SN-38 suspensions and Na_2GA/SN-38-UM because Na_2GA/SN-38-BM can be better absorbed by tumors and had longer blood circulation time, which can kill tumor cells more effectively. In summary, the new formulation Na_2GA/SN-38-BM using mechanical ball milling is feasible, portable, and environment-friendly and may be a promising formulation of SN-38 in antitumor therapy.

Acknowledgment

This work was supported by grants from the National Natural Science Foundation of China (no. 21506192) and the Zhejiang Provincial Natural Science Foundation of China (no. LY16E030010).

Disclosure

The authors report no conflicts of interest in this work.

References

1. Jaxel C, Kohn KW, Wani MC, Wall ME, Pommier Y. Structure-activity study of the actions of camptothecin derivatives on mammalian topoisomerase I: evidence for a specific receptor site and a relation to antitumor activity. *Cancer Res*. 1989;49(6):1465–1469.
2. Bissery MC, Vrignaud P, Lavelle F, Chabot GG. Experimental antitumor activity and pharmacokinetics of the camptothecin analog irinotecan (CPT-11) in mice. *Anticancer Drugs*. 1996;7(4):437–460.
3. Slatter JG, Su P, Sams JP, Schaaf LJ, Wienkers LC. Bioactivation of the anticancer agent CPT-11 to SN-38 by human hepatic microsomal carboxylesterases and the in vitro assessment of potential drug interactions. *Drug Metab Dispos*. 1997;25(10):1157–1164.
4. Iyer L, Hall D, Das S, et al. Phenotype-genotype correlation of in vitro SN-38 (active metabolite of irinotecan) and bilirubin glucuronidation in human liver tissue with UGT1A1 promoter polymorphism. *Clin Pharmacol Ther*. 1999;65(5):576–582.
5. Iyer L, King CD, Whitington PF, et al. Genetic predisposition to the metabolism of irinotecan (CPT-11). Role of uridine diphosphate glucuronosyltransferase isoform 1A1 in the glucuronidation of its active metabolite (SN-38) in human liver microsomes. *J Clin Invest*. 1998;101(4):847–854.
6. Zhang JA, Xuan T, Parmar M, et al. Development and characterization of a novel liposome-based formulation of SN-38. *Int J Pharm*. 2004;270(1–2):93–107.
7. Roger E, Lagarce F, Benoit JP. Development and characterization of a novel lipid nanocapsule formulation of SN38 for oral administration. *Eur J Pharm Biopharm*. 2011;79(1):181–188.
8. Sapra P, Zhao H, Mehlig M, et al. Novel delivery of SN38 markedly inhibits tumor growth in xenografts, including a camptothecin-11-refractory model. *Clin Cancer Res*. 2008;14(6):1888–1896.
9. Yellepeddi VK, Vangara KK, Palakurthi S. In vivo efficacy of PAMAM-Dendrimer-Cisplatin complexes in SKOV-3 xenografted BALB/c nude mice. *J Biotechnol Biomater*. 2;13:003.
10. Vangara KK, Liu JL, Palakurthi S. Hyaluronic acid-decorated PLGA-PEG nanoparticles for targeted delivery of SN-38 to ovarian cancer. *Anticancer Res*. 2013;33(6):2425–2434.
11. Sadzuka Y, Takabe H, Sonobe T. Liposomalization of SN-38 as active metabolite of CPT-11. *J Control Release*. 2005;108(2–3):453–459.
12. Gu Q, Xing JZ, Huang M, He C, Chen J. SN-38 loaded polymeric micelles to enhance cancer therapy. *Nanotechnology*. 2012;23(20):205101.
13. Carie A, Rios-Doria J, Costich T, et al. IT-141, a polymer micelle encapsulating SN-38, induces tumor regression in multiple colorectal cancer models. *J Drug Deliv*. 2011;2011(1–2):1–9.
14. Zhao H, Rubio B, Sapra P, et al. Novel prodrugs of SN38 using multiarm poly(ethylene glycol) linkers. *Bioconjug Chem*. 2008;19(4):849–859.
15. Kurzrock R, Goel S, Wheler J, et al. Safety, pharmacokinetics, and activity of EZN-2208, a novel conjugate of polyethylene glycol and SN38, in patients with advanced malignancies. *Cancer*. 2012;118(24):6144–6151.
16. Meyer-Losic F, Nicolazzi C, Quinonero J, et al. DTS-108, a novel peptidic prodrug of SN38: in vivo efficacy and toxicokinetic studies. *Clin Cancer Res*. 2008;14(7):2145–2153.
17. Serafino A, Zonfrillo M, Andreola F, et al. CD44-targeting for antitumor drug delivery: a new SN-38-hyaluronan bioconjugate for locoregional treatment of peritoneal carcinomatosis. *Curr Cancer Drug Targets*. 2011;11(5):572–585.
18. Su X, Wu L, Hu M, et al. Glycyrrhizic acid: a promising carrier material for anticancer therapy. *Biomed Pharmacother*. 2017;95:670–678.
19. Tsai YM, Chien CF, Lin LC, Tsai TH. Curcumin and its nano-formulation: the kinetics of tissue distribution and blood-brain barrier penetration. *Int J Pharm*. 2011;416(1):331–338.
20. Polyakov NE, Leshina TV. Glycyrrhizic acid as a novel drug delivery vector: synergy of drug transport and efficacy. *Open Conf Proc J*. 2011;2(1):64–72.
21. Piper JT, Singhal SS, Salameh MS, et al. Mechanisms of anticarcinogenic properties of curcumin: the effect of curcumin on glutathione linked detoxification enzymes in rat liver. *Int J Biochem Cell Biol*. 1998;30(4):445–456.

22. Vangara KK, Ali HI, Lu D, et al. SN-38-cyclodextrin complexation and its influence on the solubility, stability, and in vitro anticancer activity against ovarian cancer. *AAPS PharmSciTech*. 2014;15(2):472–482.
23. Liu H, Wang Y, Wang M, Xiao J, Cheng Y. Fluorinated poly (propylenimine) dendrimers as gene vectors. *Biomaterials*. 2014;35(20): 5407–5413.
24. Yellepeddi VK, Vangara KK, Kumar A, Palakurthi S. Comparative evaluation of small-molecule chemosensitizers in reversal of cisplatin resistance in ovarian cancer cells. *Anticancer Res*. 2012;32(9):3651–3658.
25. Kumar A, Yellepeddi VK, Vangara KK, Strychar KB, Palakurthi S. Mechanism of gene transfection by polyamidoamine (PAMAM) dendrimers modified with ornithine residues. *J Drug Target*. 2011;19(9):770–780.
26. Jwala J, Boddu SHS, Shah S, et al. Ocular sustained release nanoparticles containing stereoisomeric dipeptide prodrugs of acyclovir. *J Ocul Pharmacol Ther*. 2011;27(2):163–172.
27. Mamot C, Drummond DC, Noble CO, et al. Epidermal growth factor receptor–targeted immunoliposomes significantly enhance the efficacy of multiple anticancer drugs in vivo. *Cancer Res*. 2005;65(24):11631–11638.
28. Zhang H, Hollis CP, Zhang Q, Li T. Preparation and antitumor study of camptothecin nanocrystals. *Int J Pharm*. 2011;415(1–2):293–300.
29. Landesman-Milo D, Ramishetti S, Peer D. Nanomedicine as an emerging platform for metastatic lung cancer therapy. *Cancer Metastasis Rev*. 2015;34(2):291–301.
30. Yoshioka K, Sakai E, Daimon M, Kitahara A, et al. Role of steric hindrance in the performance of Superplasticizers for Concrete. *J Am Ceram Soc*. 1997;80(10):2667–2671.
31. Bala V, Rao S, Boyd BJ, Prestidge CA. Prodrug and nanomedicine approaches for the delivery of the camptothecin analogue SN38. *J Control Release*. 2013;172(1):48–61.
32. Tang XJ, Han M, Yang B, et al. Nanocarrier improves the bioavailability, stability and antitumor activity of camptothecin. *Int J Pharm*. 2014; 477(1–2):536–545.
33. Chu C, Abbara C, Tandia M, et al. Cetuximab increases concentrations of irinotecan and of its active metabolite SN-38 in plasma and tumour of human colorectal carcinoma-bearing mice. *Fundam Clin Pharmacol*. 2014;28(6):652–660.
34. des Rieux A, Fievez V, Garinot M, Schneider YJ, Préat V. Nanoparticles as potential oral delivery systems of proteins and vaccines: a mechanistic approach. *J Control Release*. 2006;116(1):1–27.
35. Veber DF, Johnson SR, Cheng HY, et al. Molecular properties that influence the oral bioavailability of drug candidates. *J Med Chem*. 2002;45(12):2615–2623.
36. Polyakov NE, Kispert LD. Water soluble biocompatible vesicles based on polysaccharides and oligosaccharides inclusion complexes for carotenoid delivery. *Carbohydr Polym*. 2015;128:207–219.